

# Surface Mechanics

## Group 1

Thijs Rikkerink (3259293)  
Rick Assink (3263657)  
Oriol Jo López (3759431)

September-November 2025

## **Abstract**

The experiments in this report are part of the surface functionalization process. The report describes this functionalization process by connecting the choices made during the modification process to the resulting surface behavior. Using laser texturing, optical and confocal microscopy, and contact angle measurement, data was gathered to describe the surface properties and parameters. The resulting surface is one with deep, steep troughs, showing a relatively lower wettability for high polarity liquids, but a very high wettability for low polarity liquids, as these can flow into the valleys, conforming to the Wenzel model.

# Contents

<b>1</b>	<b>Introduction</b>	<b>1</b>
<b>2</b>	<b>Materials and Methods</b>	<b>1</b>
2.1	Laser Processing . . . . .	1
2.1.1	Experimental Setup . . . . .	1
2.1.2	Pre-Lab Computations . . . . .	2
2.2	Roughness Measurements . . . . .	3
2.2.1	Experimental Setup . . . . .	3
2.3	Contact Angle Measurement . . . . .	4
2.3.1	Experimental Setup . . . . .	4
<b>3</b>	<b>Results</b>	<b>5</b>
3.1	Laser Processing . . . . .	5
3.2	Roughness Measurement . . . . .	6
3.2.1	Surface Parameters . . . . .	6
3.2.2	Roughness Values . . . . .	7
3.3	Contact Angle Measurement . . . . .	8
<b>4</b>	<b>Discussion</b>	<b>10</b>
<b>5</b>	<b>Conclusion</b>	<b>10</b>
<b>A</b>	<b>Light Conversion Carbide's parameters calculation</b>	<b>12</b>
<b>B</b>	<b>Matlab's Surface Designs</b>	<b>12</b>
<b>C</b>	<b>Calculating Surface Parameters</b>	<b>13</b>
<b>D</b>	<b>Contact Angle Measurement Setup</b>	<b>13</b>
<b>E</b>	<b>r-value calculation</b>	<b>14</b>
<b>F</b>	<b>Calculating Surface Energies</b>	<b>14</b>
<b>G</b>	<b>Uncertainty Calculations</b>	<b>15</b>
<b>H</b>	<b>Memorable Moments</b>	<b>16</b>

# 1 Introduction

This report contains the results and methods obtained and used for texturing, measuring and computing the energy of a surface. It starts off with laser texturing, which is done by ablating material from a highly polished stainless steel specimen, realizing a digitally created surface pattern. After this, the achieved surface roughness & parameters are measured using both optical and confocal microscopes. These parameters are then used to calculate the surface energy with two different liquids: de-ionized water and diiodomethane. The results from all these experiments and computations are reported in detail, with their relevant errors taken into account. The goal of this report is to describe in detail the process of surface functionalization. Modifying a surface is useful for changing the surface dependent properties of a system, such as friction, wetting and corrosion. This report will delve more specifically into the wetting part, by calculating the surface energy of the textured surface. The expected result of the surface modification in this report is a surface with a noticeably different surface energy from the untextured surface.

## 2 Materials and Methods

### 2.1 Laser Processing

In this section the setup and calculations for the laser texturing practical are reported, which includes the settings of the laser, the specimen description, lab conditions, and the utilized equipment.

#### 2.1.1 Experimental Setup

For the laser surface texturing practical assignment, a specimen of stainless steel grade X5CrNiMo17-12-2 (AISI 316) was machined using a Carbide laser system from Light Conversion, an ultra-short pulsed laser source. The wavelength of the emitted radiation was converted to the ultraviolet range by means of an harmonic generator and subsequently guided from the source to a galvanometric scanner through a series of mirrors. The Galvo-scanner was coupled to an F-theta telecentric focusing lens, which directed the laser beam onto the specimen positioned on a sample holder mounted on an XY-translation stage, itself located on a vibration-isolated optical table. The Galvo-scanner and F-theta lens assembly were mounted on a motorized Z-axis to allow precise adjustment of the focal plane. An exhaust system was used to remove hazardous fumes generated during laser processing.

For this type of experiment with the Light Conversion Carbide there are some parameters that need to be noted down if this experiment needs to be repeated. Those parameters are, the pulse duration ( $\tau$ ), which represents the temporal length of each laser pulse, the pulse energy (E), which corresponds to the energy delivered in a single pulse, the peak power ( $P_{av}$ ), the fluence (F), which expresses the laser energy per unit area on the specimen surface, and the repetition rate, the frequency (f), which indicates how many pulses are emitted per second, the scanning velocity (v), which determines the speed at which the laser beam moves over the surface, and the pulse-to-pulse overlap (%).

The pulse energy and fluence values were calculated by us, the calculations are in Appendix A, the value of  $P_{peak}$  and pulse-to-pulse overlap were obtained during the lab session, as explained in section 2.1.2 and the other parameters were provided by the lab's instructors. The values of those parameters will be displayed in Table 1.

Table 1: Processing parameters of experiments

Exp. n. [-]	$\tau$ [ps]	E [ $\mu$ J]	$P_{av}$ [W]	F [J/cm <sup>2</sup> ]	f [kHz]	v [m/s]	Overlap [%]
1	273	$33.717 \pm 0.700$	$2.023 \pm 0.042$	$9.477 \pm 1.399$	60	$60 * 10^{-2}$	95.2

The dimensions were determined using optical and digital microscopes. The optical microscope was a Leitz Wetzler 563011 (Rijswijk Holland, 070-3198973), The digital microscope used for the focus variation depth measurement was a Keyence VHX VH-Z100UR and the digital microscope used for the pictures was a Keyence VH-Z20R at 200x magnification.

### 2.1.2 Pre-Lab Computations

The experiment was conducted on 23 September 2025 in laboratory WH 117. Prior to commencing the procedure, the ambient conditions of the laboratory were recorded, showing a temperature of 22.3 °C and a relative humidity of 52.1 %.

The average laser power ( $P_{av}$ ) was determined using a thermopile sensor connected to a power meter. The measured maximum and minimum power values were 2.062 W and 1.981 W, respectively, resulting in an average power of 2.022 W.

A focus calibration test was then performed to identify the optimal focal position of the laser system. Using the Galvo-scanner and F-theta telecentric focusing lens, a series of parallel lines were written on the AISI 316 stainless steel specimen while the z-axis position of the sample was gradually adjusted. Each line corresponded to a different focal height. The resulting lines were examined under a microscope, and the line exhibiting the smallest width and highest sharpness was identified as corresponding to the minimum beam diameter and, therefore, the correct focus position. Based on this evaluation, the optimal focus was found at  $z = -175$  mm. Subsequently, the pulse-to-pulse overlap ( $OL$ ) was calculated according to the following expression:

$$OL = \left(1 - \frac{v}{df_p}\right) \times 100\% \quad (1)$$

where  $v$  represents the laser scanning velocity,  $d$  the beam diameter, and  $f_p$  the pulse repetition frequency. For the present configuration, the parameters were  $v = 60 \times 10^{-3} \text{ m s}^{-1}$ ,  $d = 21 \mu\text{m}$ , and  $f_p = 60 \text{ kHz}$ , yielding an overlap of 95.2%.

This high overlap value indicates a dense energy deposition on the surface, leading to a high local fluence accumulation. As a result, the processed lines are expected to be narrow, smooth, and continuous, forming deep, uniform grooves with minimal segmentation. However, this regime also increases the likelihood of thermal effects such as oxidation or material redeposition on the specimen surface.

Before the session, calculations were performed to describe the laser's parameters. Three surfaces were also prepared on Matlab, of which one was chosen to be engraved. Its parameters are described in table 2.

Table 2: Surface Parameter Settings

Crater [-]	n [-]	v [m/s]	Hatching [-]	Pitch x/y [m]	Overshoot [-]	Hatch Angle [°]	Length [-]
1	133	0.06	True	$40 * 10^{-6}$	50	90	250

This configuration was selected based on the MATLAB simulations, which can be found on appendix B, which indicated that the resulting surface pattern would likely exhibit favorable hydrophobic behavior. Several adjustments were made to this configuration in order to optimize the laser ablation process, including the use of the full available laser power (100%).

## 2.2 Roughness Measurements

In this section the setup and results for the confocal measurements of the laser textured surface are reported. This measurement was used to determine the surface parameters, such as pitch, depth and beam diameter. The confocal measurements should be more accurate than the depth variation of section 1, and should therefore allow for a higher certainty in the surface energy calculations in section 3.

### 2.2.1 Experimental Setup

The confocal measurement experiment was conducted in the Tribolab in Horst Ring N100. The microscope used for these measurements was the Sensofar S Neox [3], shown in figure 1 with the specimen. This specimen was the laser-textured specimen from Section 1. Measurements were done of the pitch, beam diameter and depth of the surface, using different magnifications and light levels. All settings used for the different scans are structured in table 4. Not all of these were saved, as some were used to get a good gauge on what settings were suitable for measuring the surface parameters. Especially the depth, which required 8 attempts to get even a few useful data points. Only scans 9, 11, 12, 14 and 15 were saved and will be analyzed in the results section of this report. The saved data was stored in the teams in the "10\_raw-data" folder and their names are shown in table 3. The resolution was set at 90 nm/pixel.



Figure 1: Confocal Measurement with Sensofar S Neox

Table 3: Saved Data

Scan	File Name
9	150x magnification data
11	150x magnification with 2 depths
12	peak measurement 50x
14	peak measurement 2 50x
15	peak measurement 3 50x

Table 4: Settings of the Confocal Scans

Scan #	Magn.	Range / T / B [μm]	Nº of Scans	Light Intensity [%]	Area Scanned [%]
1	x10	Default Setting	1	Default Setting	20
2	x10	100 / 50 / 50	1	3.66	24
3	x10	100 / 50 / 50	1	4.26	26
4	x10	250 / 50 / 200	1	4.26	40
5	x20	250 / 50 / 200	3	3.66 / 10 / 20	46
6	x20	250 / 50 / 200	3	3.66 / 20 / 40	50
7	x50	250 / 50 / 200	3	3.66 / 30 / 50	25
8	x100	150 / 50 / 100	3	9 / 35 / 60	<25
9	x150	150 / 50 / 100	3	9 / 35 / 97	25
10	x150	100 / 50 / 50	4	14 / 35 / 60 / 97	0
11	x150	100 / 50 / 50	4	14 / 35 / 60 / 97	25
12	x50	20 / 10 / 10	2	3.4 / 10.26	25
13	x150	10 / 5 / 5	1	17.70	25
14	x150	20 / 10 / 10	1	14.70	25
15	x50	20 / 10 / 10	1	14.70	25

### 2.3 Contact Angle Measurement

An important measure for a surface is wettability, the ability to maintain contact with a surface. So an experiment was performed to find the static contact angle of drops of water and diiodomethane on the specimen, using the Krüss Advance [2].

#### 2.3.1 Experimental Setup

The specimen was first cleaned using acetone and isopropyl alcohol in an ultrasonic cleaner, the sonoSwiss sw6h. 5 drops were then used for both water and diiodomethane, 2 on the flat, untextured surface and 1 on each of the 3 textured squares. Between testing both fluids the specimen was cleaned again. The contact angle results of the droplet's left side, right side, and their mean should be determined along with the temperature of the drops.

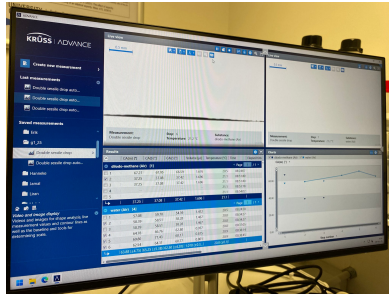


Figure 2: Contact angle measurement settings with the Krüss advance

Table 5: Experiments CA

Drop	Liquid	Location
1	Water	Flat, untextured
2	Water	Flat, untextured
3	Water	Square 1
4	Water	Square 2
5	Water	Square 3
6	Diiodomethane	Flat, untextured
7	Diiodomethane	Flat, untextured
8	Diiodomethane	Square 1
9	Diiodomethane	Square 2
10	Diiodomethane	Square 3

### 3 Results

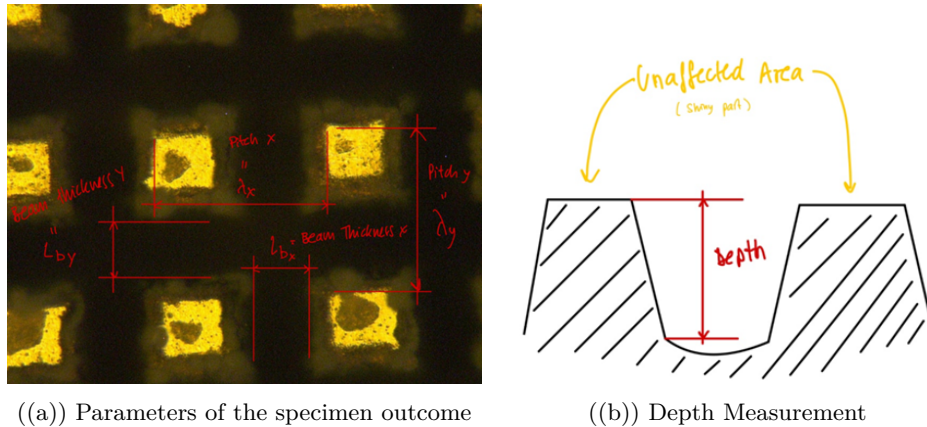
#### 3.1 Laser Processing

After the experiment the sample with its three laser textured squares was cleaned, after which the dimensions of the laser texture were measured. This was done using both an optical and digital microscope, where the optical microscope was used for the pitch and beam diameter, and the digital microscope was used for the depth measurement. The dimensions are described in table 6 and further contextualized in figure 3.

The depth which was measured using the focus variation method is far less than that of the confocal measurement. This is because the surface has very steep inclines on its peaks, which barely allows light to reflect back to the users eyes. The confocal measurement gives a better idea of the actual depth.

Table 6: Microscopy measurements of the laser textured surface

Measurand	Direction	Square 1	Square 2	Square 3
Pitch [ $\mu\text{m}$ ]	x	100	97.5	100
$\vdots$	y	95	100	97.5
Beam Thickness [ $\mu\text{m}$ ]	x	30	30	27.5
$\vdots$	y	35	30	35
Depth [ $\mu\text{m}$ ]	x	3.9	3	1
$\vdots$	y	4	3	2
$\vdots$	xy	3.5	2	4



((a)) Parameters of the specimen outcome

((b)) Depth Measurement

Figure 3: Description of the measured dimensions of the laser textured surface.

During the laboratory session, there was also time to capture a few memorable moments that will remain a record of the experience. Beyond calculations and theoretical and practical discussions, the atmosphere was relaxed and allowed for both humor and collaboration between students and instructors. This friendly yet professional environment made the laboratory work especially enjoyable and enriching. Some pictures of that session can be found in appendix H.

## 3.2 Roughness Measurement

The goal of the confocal roughness measurement was to measure the surface accurately, so that the parameters of the surface can be used to describe surface properties, such as surface energy.

### 3.2.1 Surface Parameters

Using the confocal scans, the surface parameters can be determined. In this section, the pitch and beam diameter will be derived from the 150x and 50x magnification data. Where the pitch and beam diameter are derived from is shown in figure 3.

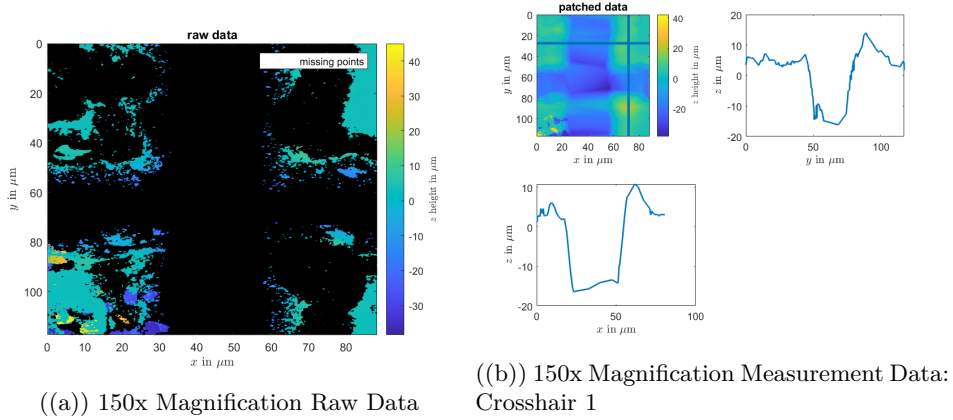


Figure 4: Square 1: 150x Magnification

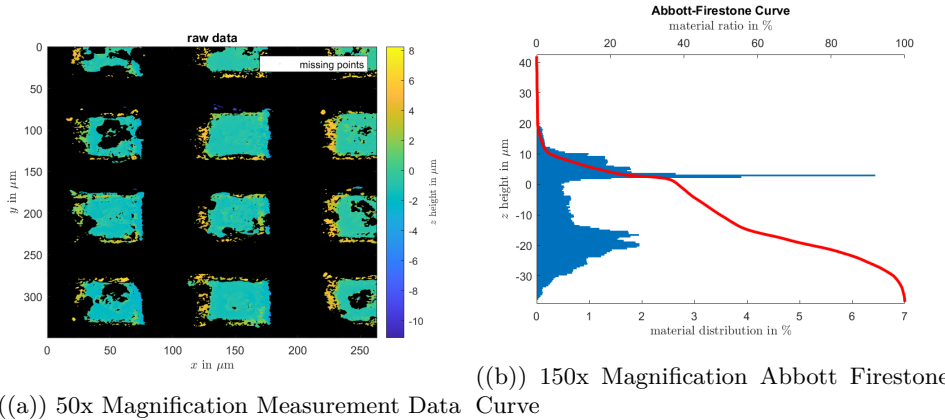


Figure 5: Square 1

From figure 4(b) the beam diameter can be read. It is important to note that this data is patched, and the depth is therefore not the actual depth, as there are only a few data points on the maximum depth and these are patched over and not all covered by the crosshair. Noting this, four different beam diameter measurements were made using different crosshair locations: the one shown in figure 4(b) and a new crosshair on the top left peak. These measurements are shown in table 7.

Table 7: Beam Diameter Measurement for Square 1: Two Crosshair Locations

<b>Measurand</b>	X 1 [ $\mu m$ ]	Y 1 [ $\mu m$ ]	X 2 [ $\mu m$ ]	Y 2 [ $\mu m$ ]	Mean [ $\mu m$ ]
<b>Value</b>	27.5447	23.3138	26.8539	23.6591	$25.3429 \pm 1.0833$

The pitch measurements are done similarly, except in the 50x magnification data. This is because there are no full peaks visible in the 150x data. The measurements for the pitch were done in figure 5(a), for different pairs of peaks in both x and y direction. All these measurements were taken between data points with a height of  $0 \pm 2 \mu m$ , to not take into account the slope from peak to valley. These measured values are displayed in table 8.

Table 8: Pitch Measurement for Squares 1, 2 & 3: Two Points

<b>Measurand</b>	X 1 [ $\mu m$ ]	Y 1 [ $\mu m$ ]	X 2 [ $\mu m$ ]	Y 2 [ $\mu m$ ]	Mean [ $\mu m$ ]
<b>Square 1</b>	102.685	98.568	102.428	100.884	$101.141 \pm 0.9455$
<b>Square 2</b>	108.604	98.053	102.170	100.883	$102.428 \pm 2.2312$
<b>Square 3</b>	109.376	94.707	101.399	102.171	$101.913 \pm 2.9994$

*Note 1:* Examples of the measured points for the peaks and beam diameter are shown in appendix C.

*Note 2:* The uncertainty calculations are described in appendix G.

### 3.2.2 Roughness Values

The confocal measurement data was processed to the following roughness data. The 150x magnification data in table 9 gives a better representation of the roughness parameters, as it was measured with multiple light levels, many scanning planes and a higher magnification. As seen in the surface figures in section 3.2.1, the 50x magnification has very few data points in the valleys. This is because these were measured to obtain the pitch, which does not require deep data points. The surface which was scanned has very deep, steep troughs as illustrated in figure 6. This makes it hard to get both non-overexposed data from the peaks and readable data from the valleys. Since only the 150x data has data points in both the peaks and valleys, the depth of the surface of square 1 is assumed to be that of this 150x data, resulting in:  $S_z = 80.610 \pm 0.51 \mu m$  [9]

As there is no 150x data from squares 2 and 3 due to time constraints, their data is only used for the pitch in section 3.2.1.

Table 9: Roughness Values Square 1, 2 & 3: 50x & 150x Magnification (Unit: [ $\mu m$ ] U.N.O.)

<b>Parameter</b>	$S_a$	$S_{mean}$	$S_q$	$S_p$	$S_v$	$S_{sk}$	$S_{ku}$	$S_z$	$S_t$	$u_{\bar{x}} [\%]$
<b>Sq 1: 150x</b>	12.330	-6.520	14.423	44.151	36.749	0.149	2.031	80.610	80.900	0.63%
<b>Sq 1: 50x</b>	2.669	0.408	3.288	8.002	11.466	-0.041	2.601	19.404	19.468	0.65%
<b>Sq 2: 50x</b>	2.173	0.321	2.759	9.194	10.232	-0.127	3.286	19.342	19.426	0.65%
<b>Sq 3: 50x</b>	2.037	0.314	2.620	8.373	9.287	0.170	3.179	17.448	17.660	0.65%

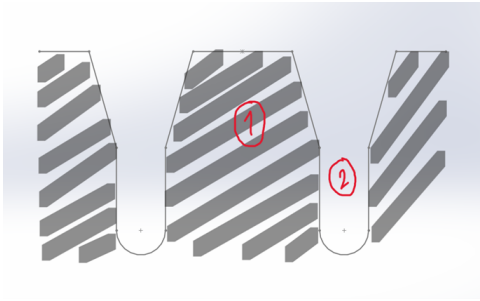


Figure 6: Illustration of the laser textured surface.

### 3.3 Contact Angle Measurement

After performing the contact angle measurement discussed in chapter 2.3 the results were determined, and shown in table 10 and 11.

Table 10: Contact angle measurements water

Drop	Location	$\theta_l$ [°]	$\theta_r$ [°]	$\theta_m$ [°]	V [ $\mu L$ ]	T [°C]
1	Flat	58.51	58.28	58.39	1.467	$20.8 \pm 0.058$ °C
2	Flat	58.13	55.2	56.67	1.302	$21.2 \pm 0.058$ °C
3	Sqr 1	66.76	62.80	64.78	0.957	$20.8 \pm 0.058$ °C
4	Sqr 2	71.43	68.17	69.80	0.815	$20.9 \pm 0.058$ °C
5	Sqr 3	64.31	60.77	62.54	0.801	$20.9 \pm 0.058$ °C

Table 11: Contact angle measurements diiodomethane

Drop	Location	$\theta_l$ [°]	$\theta_r$ [°]	$\theta_m$ [°]	V [ $\mu L$ ]	T [°C]
1	Flat	37.08	37.42	37.25	1.696	$21.1 \pm 0.058$ °C
2	Flat	35.21	35.51	35.36	1.596	$21.2 \pm 0.058$ °C
3	Sq 1	-	-	-	-	$21.1 \pm 0.058$ °C
4	Sq 2	-	-	-	-	$21.1 \pm 0.058$ °C
5	Sq 3	-	-	-	-	$21.2 \pm 0.058$ °C

Table 12: Contact angle measurements mean

Location	Liquid	$\theta_m$ [°]
Flat	Water	$57.53 \pm 0.862$
Flat	Diiodomethane	$36.31 \pm 0.952$
Textured	Water	$65.71 \pm 2.151$

For the contact angle of the textured surface with diiodomethane no results were found due to the complete wetting of the specimen ( $\theta_{CA} \approx 0$ ). For the flat untextured part of the specimen the assumptions of the Young's equation (equation 2) apply.

- The surface is smooth
- The surface is rigid
- The surface is homogeneous
- The surface is insoluble
- The surface is non-reactive

$$\gamma_{S(L)} + \gamma_{L(V)} \cos(\theta) = \gamma_{S(V)} \quad (2)$$

Due to the complete wetting of the surface when using diiodomethane it is assumed that the Wenzel state applies for both the water as for the diiodomethane, this means the contact angle needs to be calculated using equation 3.

$$\cos(\theta_m) = r \cdot \cos(\theta_y) \quad (3)$$

For surface energy the Owen-Wendt method was used, as the experiment was performed using water (high polarity) and diiodomethane (low polarity). The mean surface energy parameters of the liquids were determined using available data[1] and interpolation.

Table 13: Mean liquid surface energy parameters

Liquid	$\gamma_L$ [mN/m]	$\gamma_L^d$ [mN/m]	$\gamma_L^p$ [mN/m]
Water	$72.7 \pm 0.0093$	$27.20 \pm 0.0005$	$45.46 \pm 0.0088$
Diiodo-methane	$50.68 \pm 0.0060$	$50.68 \pm 0.0060$	0

$$\gamma = \gamma^d + \gamma^p \quad (4)$$

$$\frac{\gamma_L(1 + \cos\theta)}{2\sqrt{\gamma_L^d}} = \sqrt{\gamma_S^p} \frac{\sqrt{\gamma_L^p}}{\sqrt{\gamma_L^d}} + \sqrt{\gamma_S^d} \quad (5)$$

Using these equations the mean surface energies of the flat untextured part, and the textured part were determined (see appendix F).

Table 14: Mean solid surface energy parameters

Location	$\gamma_S^d$ [mN/m]	$\gamma_S^p$ [mN/m]	$\gamma_S$ [mN/m]
Flat	$41.32 \pm 1.25$	$11.02 \pm 0.33$	$52.34 \pm 1.58$
Textured	$50.68 \pm 1.66$	$0.57 \pm 0.02$	$51.25 \pm 1.68$

## 4 Discussion

Due to the deep, barely measurable valley of the surface, the optical microscopy was not able to get a good gauge of the depth. This was partially achieved by the confocal microscopy, after some tinkering with light and step settings. Resulting from this, the depth measured using the depth variation [6] was around  $3\text{-}4 \mu\text{m}$ , where the confocal measurement [9] put it at a more accurate  $80\text{-}81 \mu\text{m}$ . The depth and beam diameter of these two measurement methods lie very close however, which means these are reliable results.

The 50x magnification roughness parameters in table 9 are not reliable, as there are virtually no data points in the valleys. This was because these pictures [5(a)] were taken to only measure the pitch. The 150x magnification data is the only one to be used for roughness, beam and depth parameters. As there are no other 150x scans, the data seems accurate but is not replicable per say. This seeps through into the surface energy parameters, as their calculations are partially based on the roughness parameters.

The contact angle measurements in tables 10 and 11 are likely reliable data, as they were tested on all textured squares, as well as the untextured part of the specimen. The results of the surface energy calculation shows some interesting behavior, as the total surface energy is essentially unchanged between the flat, untextured surface and the textured surface, the textured surface however, is reported to be almost entirely dispersive. This is a result of the complete wetting behavior of the textured part with diiodomethane, so a useful static contact angle could not be determined.

## 5 Conclusion

In this report the stainless steel specimen was laser-engraved to obtain a symmetrical, gridded surface. This surface was then measured with several microscopes, to obtain its parameters. Here it was immediately noticed that the surface had a relatively high depth for its pitch, resulting in deep troughs that would barely reflect light. This made the depth measurement significantly more difficult than expected. Eventually some data for all these parameters was obtained, which was used to calculate the surface energy. During the droplet experiment however, it was noticed that the diiodomethane drops fully wetted the textured surface, making it impossible to get a contact angle measurement from it. Due to this complete wetting of the surface the surface energy results of the polar/dispersive split are unreliable. It can be concluded that the surface is sufficiently wetting for diiodomethane, and the total surface energy is essentially the same. This is an unexpected result, as a noticeably smaller total surface energy was expected, with less wetting.

In future experiments, it would be wise to texture the surface differently, e.g. with a higher pitch-depth ratio, as to simplify and streamline the roughness measurements and therefore obtain more accurate results. Using literature to guide the surface design is also wise, to ensure that the contact angle for all liquids is measurable, which would lead to more accurate surface energy parameters as well.

## References

- [1] Jikan Surface Nano-Engineering Company. Table of polar and dispersive components of liquid surface tension. URL <https://www.jikangroup.com/2021/10/17/polar-dispersive-liquid-surface-tensions/>.
- [2] krüss scientific. Drop shape analyzer dsa100 specifications. URL <https://www.kruss-scientific.com/files/kruss-techdata-dsa100-en.pdf>.
- [3] Sensofar Metrology. Non-contact 3d optical profiler s neox. URL <https://www.sensofar.com/wp-content/uploads/2015/10/Brochure-S-neox-v6-EN-web.pdf>.

## A Light Conversion Carbide's parameters calculation

In this section will be the calculations made to obtain the values of pulse energy and fluence, as well as the uncertainties that were involved during the calculation.

The pulse energy value was obtained with the following formula, which was taken from the laboratory session assignments.

$$E = \frac{P_{peak}}{f} = \frac{2.023 \pm 0.042W}{60kHz} = 33.717 \pm 0.700\mu J \quad (6)$$

The formula used for the fluence value was obtained from the same section as the pulse energy, and is the following one.

$$F = \frac{E}{\pi r^2} \quad (7)$$

The parameter  $r$  is the laser's beam radius in focus location, which is obtained by dividing by 2 the laser's beam diameter, also provided by the wording of Assignment 2, its value is  $15.05 \pm 1.1\mu m$ .

For the fluence's standard deviation calculation it needs to be taken into account the fact that the beam's radius has two mathematical operations - has a power of 2, and multiplication by constant  $\pi$ . So, the outcome of this is the following.

$$F = \frac{33.717\mu J}{\pi \times (15.05\mu m)^2} \times 2 = 9.477J/cm^2 \quad (8)$$

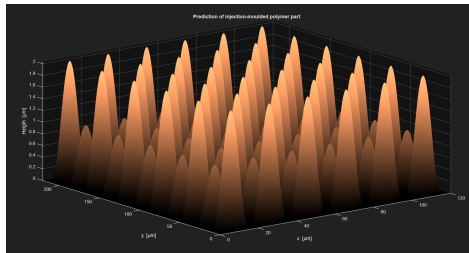
$$\Delta F = F \times \sqrt{\left(\frac{\Delta E}{E}\right)^2 + \left(\frac{\pi \times \Delta r}{\pi \times r^2}\right)^2} \quad (9)$$

$$\Delta F = 9.477 \frac{J}{cm^2} \times \sqrt{\left(\frac{0.700\mu J}{33.717\mu J}\right)^2 + \left(\frac{\pi \times ((15.05\mu m)^2 \times 2 \times \frac{1.1\mu m}{15.05\mu m})}{\pi \times (15.05\mu m)^2}\right)^2} = 1.399 \frac{J}{cm^2} \quad (10)$$

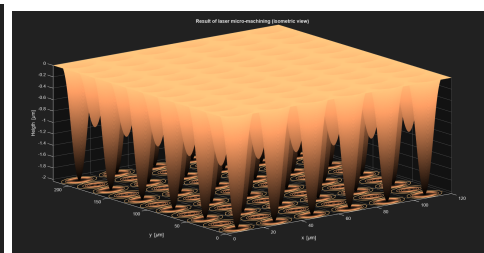
Then, the fluence has a value of  $9.477 \pm 1.399 \frac{J}{cm^2}$

## B Matlab's Surface Designs

The following figures are images extracted from a Matlab script provided by the teaching staff in the laboratory, which was uploaded on Canvas. These figures are the simulation of the surface outcome once the laser had finished its process.



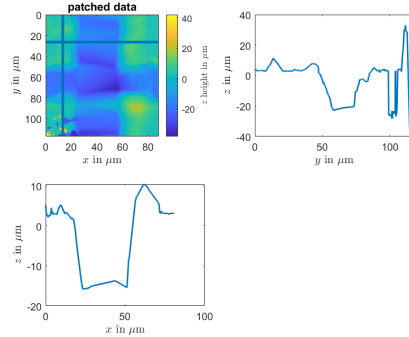
((a)) Surface simulation outcome



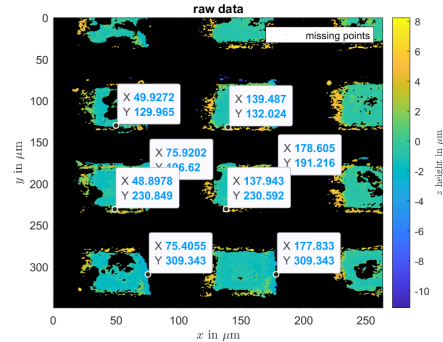
((b)) Laser micro-machining

## C Calculating Surface Parameters

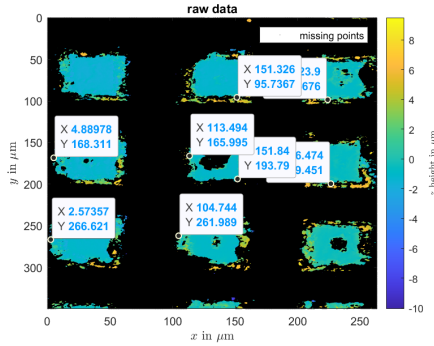
In this appendix section the figures used to compute the beam diameter and pitch are displayed.



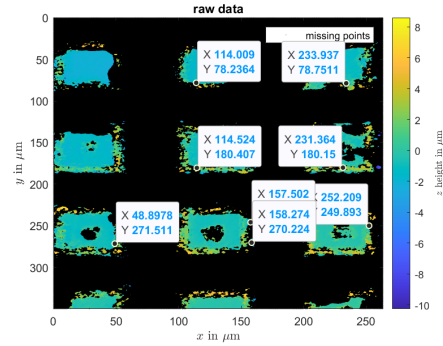
((a)) 150x Magnification Measurement Data:  
Crosshair 2



((b)) Pitch measurement: square 1 points



((a)) Pitch measurement: square 2 points



((b)) Pitch measurement: square 3 points

## D Contact Angle Measurement Setup

In figure 10 a picture of how the specimen was placed in the Krüss Advance for contact angle measurement is shown.

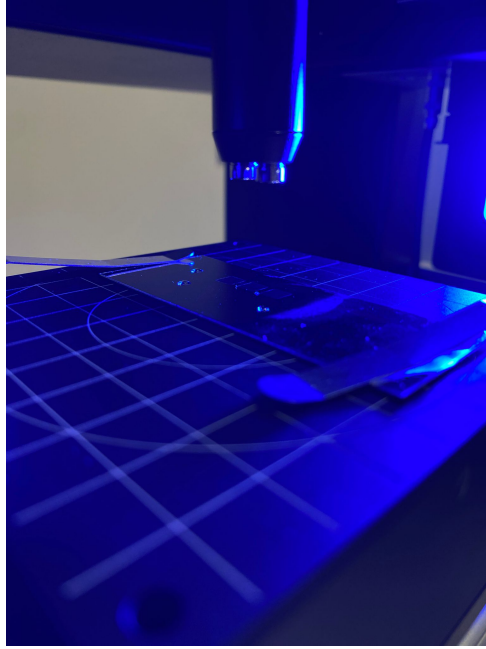


Figure 10: Contact angle measurement setup

## E r-value calculation

To determine the static contact angle on the textured parts, the Wenzel state is assumed.

$$\cos(\theta_m) = r \cdot \cos(\theta_y) \quad (11)$$

For this, the r-value needs to be determined.

$$r = \frac{\text{Actual area}}{\text{Projected area}} \quad (12)$$

Using the mean value of the results from table 8;  $101.83 \mu\text{m}$ . With this the projected area could be determined:

$$\text{Projected area} = \text{Pitch}^2 = 10368.8 \mu\text{m}^2 \quad (13)$$

Due to limited data found for the depth measurements, it is assumed that the surface consists of perfectly square cross-section pillars, with height (or depth of valleys)  $80.6 \mu\text{m}$  and width of the pillars  $50 \mu\text{m}$ . With these assumptions the actual area could be calculated:

$$\text{Actual area} = \text{Projected area} + 4 \cdot (d_{valley} * w_{pillar}) = 26488.8 \mu\text{m}^2 \quad (14)$$

Using this to calculate r:

$$r = \frac{26488.8}{10368.8} = 2.55 \quad (15)$$

## F Calculating Surface Energies

To calculate the surface energies of the specimen, untextured and textured, the values of table 13 were used alongside the mean of the measured  $\theta_m$ . For the diiodomethane on the flat untextured part this means:

$$\frac{50.68(1 + \cos(36.31^\circ))}{2\sqrt{50.68}} = \sqrt{\gamma_{S,flat}^p} \frac{\sqrt{0}}{\sqrt{50.68}} + \sqrt{\gamma_{S,flat}^d} \quad (16)$$

$$\left(\frac{50.68(1 + \cos(36.31^\circ))}{2\sqrt{50.68}}\right)^2 = \gamma_{S,flat}^d \quad (17)$$

$$\gamma_{S,flat}^d = 41.32 \text{mN/m} \quad (18)$$

Plugging this into equation 5 for water to find  $\gamma_{S,flat}^p$ :

$$\frac{72.7(1 + \cos(57.53^\circ))}{2\sqrt{27.20}} = \sqrt{\gamma_{S,flat}^p} \frac{\sqrt{45.46}}{\sqrt{27.20}} + \sqrt{41.32} \quad (19)$$

$$10.71 = 1.29 \sqrt{\gamma_{S,flat}^p} + 6.43 \quad (20)$$

$$\gamma_{S,flat}^p = 11.02 \text{mN/m} \quad (21)$$

The total surface energy for the untextured part can then be calculated:

$$\gamma_{S,flat} = \gamma_{S,flat}^d + \gamma_{S,flat}^p = 41.32 + 11.02 = 52.34 \text{mN/m} \quad (22)$$

For the textured part equation 3 and the r-value from appendix E was used to find the static contact angle.

$$\cos(65.71^\circ) = 2.55 \cdot \cos(\theta_y) \quad (23)$$

$$\theta_y = \cos^{-1}\left(\frac{\cos(65.71^\circ)}{2.55}\right) = 80.72^\circ \quad (24)$$

The angle for diiodomethane was measured as 0 for the textured surface:

$$\frac{50.68(1 + \cos(0^\circ))}{2\sqrt{50.68}} = \sqrt{\gamma_{S,text}^p} \frac{\sqrt{0}}{\sqrt{50.68}} + \sqrt{\gamma_{S,text}^d} \quad (25)$$

$$\left(\frac{50.68(1 + \cos(0^\circ))}{2\sqrt{50.68}}\right)^2 = \gamma_{S,text}^d \quad (26)$$

$$\gamma_{S,text}^d = 50.68 \text{mN/m} \quad (27)$$

Plugging this into equation 5 for water using the new angle to find  $\gamma_{S,text}^p$ :

$$\frac{72.7(1 + \cos(80.72^\circ))}{2\sqrt{27.20}} = \sqrt{\gamma_{S,text}^p} \frac{\sqrt{45.46}}{\sqrt{27.20}} + \sqrt{50.68} \quad (28)$$

$$8.09 = 1.29 \sqrt{\gamma_{S,text}^p} + 7.12 \quad (29)$$

$$\gamma_{S,text}^p = 0.57 \text{mN/m} \quad (30)$$

The total surface energy for the untextured part can then be calculated:

$$\gamma_{S,text} = \gamma_{S,text}^d + \gamma_{S,text}^p = 50.68 + 0.57 = 51.25 \text{mN/m} \quad (31)$$

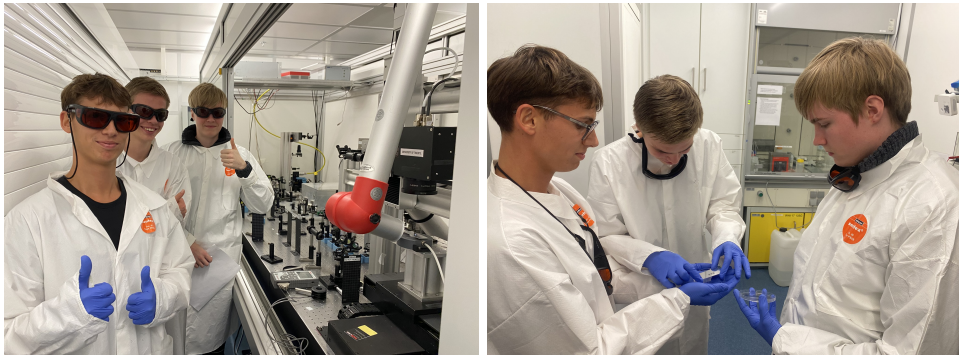
## G Uncertainty Calculations

Uncertainty calculations for the surface & roughness parameters, and contact angle measurements. In the uncertainty budget in table 15 the most relevant influencing factors are displayed, after which the type A and type B uncertainties are calculated and combined using the quadrature rule into combined standard uncertainties, which are shown next to their relevant mean values in the report.

Table 15: Sources of Uncertainty

Influencing Factor	Error type	Distribution	Error value
1.1: Confocal Measurement (Sensofar S-Neox) [3]			
Optical resolution 50x	B	Uniform	$\pm 0.17 \mu m$
Optical resolution 150x	B	Uniform	$\pm 0.14 \mu m$
Step height repeatability	B	Uniform	0.1 %
Step height accuracy	B	Gaussian	0.5 %
1.2: Contact angle measurement (Krüss advance) [2]			
Software-based resolution	B	Uniform	$\pm 0.0058 \mu m$
Software-based accuracy	B	Uniform	$\pm 0.058 \mu m$
Temperature resolution	B	Uniform	$\pm 0.058 ^\circ C$
2.1: Interpreting the surface plot figures			
Repeated measurement Sq 1 150x	A	Gaussian	$\pm 1.0833 \mu m$
Repeated measurement Sq 1 50x	A	Gaussian	$\pm 0.9455 \mu m$
Repeated measurement Sq 2 50x	A	Gaussian	$\pm 2.2312 \mu m$
Repeated measurement Sq 3 50x	A	Gaussian	$\pm 2.9994 \mu m$
2.2: Interpreting the contact angle measurements			
Repeated measurement flat, diiodomethane	A	Gaussian	$\pm 0.95 ^\circ$
Repeated measurement flat, water	A	Gaussian	$\pm 0.86 ^\circ$
Repeated measurement textured, water	A	Gaussian	$\pm 2.15 ^\circ$

## H Memorable Moments



((a)) Checking on the laser ablation process

((b)) Specimen's Storage

Figure 11: Memorable moments from the laser texturing laboratory session.